Int. J. Heat Mass Transfer. Vol. 21, pp. 1099–1109

0017-9310/78/0801-1099 $02.00/0

A PERIODIC INTERMITTENT MODEL FOR THE WALL REGION OF A TURBULENT BOUNDARY LAYER

F. G. VAN DONGEN, A. C. M. BELJAARS and D. A. DE VRIES
Laboratory for Fluid Dynamics and Heat Transfer, Department of Technical Physics,
Eindhoven University of Technology, Postbus 513, Eindhoven, Netherlands

(*Received* 6 *July* 1977)

Abstract—Visualisation studies of turbulent flow in the vicinity of a wall have shown that short time intervals with strong turbulent activity (so-called bursts and sweeps) alternate with intervals of a much longer duration, during which viscous effects predominate. These phenomena show a quasi-periodicity in space and time. The evolution of the velocity and temperature profiles is calculated for one time period from two-dimensional laminar boundary-layer equations for the region $0 < y^+ < 40$. The combined effect of a burst and sweep is thought to give rise to uniform velocity and temperature profiles at the beginning of a period. In this respect the present model is similar to the surface renewal model. The various parameters occurring in the equations and their boundary conditions are derived from experiment. The model predicts the velocity and temperature profiles in the wall region and the fluxes of heat and momentum at the wall reasonably well.

NOMENCLATURE

a, thermal diffusivity [m^2/s];
a_1, a_2, coefficients in power series;
c_p, specific heat at constant pressure [$J/(kg\,K)$];
f, stream function for the convected sub-boundary layer;
g, dimensionless temperature for the convected sub-boundary layer;
n, number ($\pm 1, \pm 2, \ldots$);
p, pressure [Pa];
Pr, Prandtl number $= \nu/a$;
q, heat flux density [W/m^2];
Re_{δ_2}, Reynolds number $= U_\infty \delta_2/\nu$;
t, time [s];
T, period [s];
u, velocity component in x-direction [m/s];
u^+, dimensionless value of u ($= u/v^*$);
v, velocity component in y-direction [m/s];
v^*, friction velocity [m/s];
w, velocity component in z-direction [m/s];
x, coordinate in main flow direction, parallel to wall [m];
y, coordinate perpendicular to wall [m];
y^+, dimensionless coordinate ($= yv^*/\nu$);
z, coordinate parallel to wall, perpendicular to main flow direction [m].

Greek symbols

β, γ, integration constants;
δ, boundary-layer thickness [m];
δ_2, momentum loss thickness [m];
η, similarity coordinate;
θ, temperature [K];
θ^*, friction temperature ($= q_w/\rho c_p v^*$) [K];
λ, thermal conductivity [$W/(m\,K)$];
$\lambda_{x,z}$, wave length [m];
μ, dynamic viscosity [$kg/(m\,s)$];
ν, kinematic viscosity [m^2/s];
ρ, specific mass [kg/m^3];
τ, shear stress [Pa].

Subscripts

b, burst;
c, convective;
i, instability;
0, initial value, inner solution;
w, wall;
∞, free stream value, outer solution.

1. INTRODUCTION

MANY experiments on the mechanism of turbulent exchange of mass and momentum in the wall region of a turbulent boundary layer have revealed that the exchange processes are characterized by their intermittency and quasi-periodicity. We refer to the visualization studies of Kline *et al.* [1, 2] and Corino and Brodkey [3]. Their visualization studies have shown the existence of recognizable flow patterns in the wall region, which repeat themselves with time intervals that are randomly spread around an average, called the burst period. The sequence of events during one such interval can be divided in two stages:

1. A stage, characterized by its small velocity fluctuations and a gradual deceleration of the fluid near the wall.
2. A stage with fast and violent velocity fluctuations so-called burst and sweep event.

The duration of the second stage is much smaller than that of the first one. Kline *et al.* and Corino and Brodkey describe this stage as follows. During a small time interval, there is an intensive exchange of momentum between the wall region and regions further from the wall as a consequence of fast and violent velocity fluctuations. First a burst appears, i.e. a flow module, consisting of a combination of negative velocity fluc-

tuations, in the main flow direction, u', and positive velocity fluctuations in a direction perpendicular to the wall, v'. Low momentum fluid is ejected from the wall region. The burst is succeeded by a sweep, a combination of velocity fluctuations $u' > 0$ and $v' < 0$, which brings high momentum fluid into the wall region. This fluid is then gradually decelerated, until the next cycle of events is set in by a new burst. The appearance of bursts and sweeps can be interpreted as local instabilities in the wall region, which can be supported by two facts, adopted from the visualization studies:

1. During a burst a fast and abrupt growth of the velocity fluctuations is observed, being an essential feature of instabilities.

2. The velocity profile $u(y,t)$ just before a burst always contains an inflexional zone at $y^+ = 20$–30, indicating the possibility of an instability.

The discussed sequence of events is shown in Fig. 1.

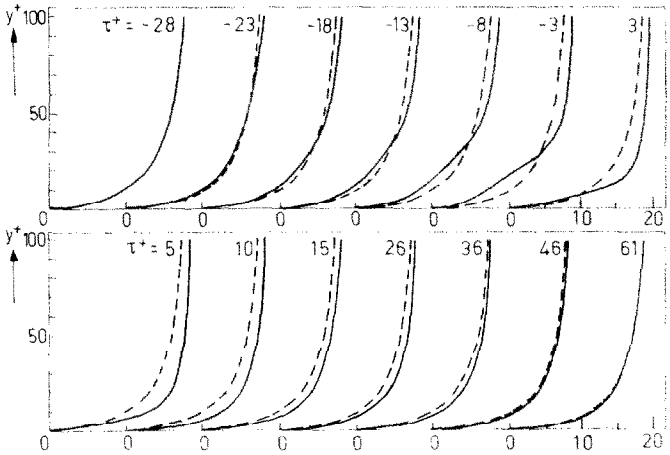

FIG. 1. Instantaneous velocity profiles $u(y^+, \tau^+)/v^*$ in the wall region (——), obtained via a conditional averaging scheme after Blackwelder and Kaplan [7], and the time averaged velocity profiles (-----). $\tau^+ = v^{*2}\tau/\nu$ is the dimensionless time with respect to the occurrence of a burst. $Re_\delta = 2550$.

The visualization studies of Kline *et al.* have demonstrated another important feature of the flow field in the wall region, i.e. a "streak"-structure, apparent in a plane parellel to the wall at heights $0 < y^+ < 40$. These longitudinal "streaks" can be viewed as regions with relatively high and low velocity components in the main flow direction. The interaction between two neighbouring "streaks" results in a weak vorticity component in the main flow-direction. One finds in the wall region pairs of counter-rotating vortices, as shown in Fig. 2.

In classical theories one derives equations for the time-averaged velocity components, pressure and temperature, making use of the Reynolds' decomposition. The visualization studies suggest that the common averaging procedure is not the most adequate one for the wall region, because it covers up the observed coherence in the wall region. The first theory, which fits very well in the discussed conceptual picture of the wall region, is the surface renewal model, independently developed by Einstein and Li [4] and Hanratty [5]. Actually this model preceded the visualization studies. It is based upon two basic assumptions:

1. The flow field, observed at a fixed position is periodical in time.

2. Turbulent exchange occurs during very short time intervals. Low momentum fluid is ejected from the wall region and replaced by high momentum fluid originating from the upper edge of the buffer region. This is the so-called surface renewal, in the visualization studies identified as the combination of a burst and sweep. Supposing that the surface renewal leads to a velocity profile $u(y) = u_0$, with constant u_0, and that the gradual distortion of this profile is caused by viscous forces only, one arrives at the following mathematical formulation of the surface renewal model:

$$\frac{\partial u}{\partial t} = \nu \frac{\partial^2 u}{\partial y^2} \text{ with } u(0,t) = 0; \quad u(y,0) = u_0. \quad (1.1)$$

The gradual deceleration after the occurrence of a burst and sweep is thus described as essentially laminar and one-dimensional.

Black [6] has given a simplified three-dimensional picture of the flow field in the wall region, incorporating the findings of the visualization studies (cf. Fig. 3). In this model local instabilities, giving rise to bursts and sweeps, are convected at a velocity U_c in the main flow direction. For fixed values of z they are separated by a distance λ_x. The region of impact extends in the z-direction over a distance λ_z. Hence a plane $y^+ = \text{constant}$, with $0 < y^+ < 40$, is divided in "streaks" with a width λ_z. In the neighbouring "streaks", one

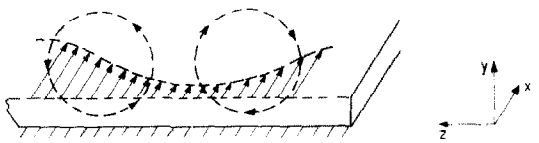

FIG. 2. A conceptual picture of the "streak"-structure in the wall region and the corresponding secondary motion.

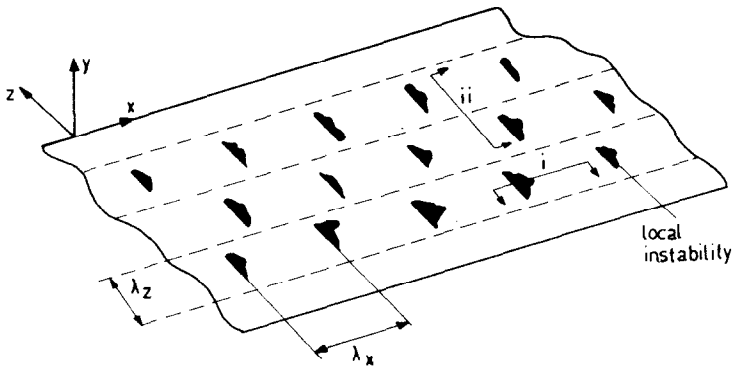

FIG. 3. A three-dimensional picture of the flow field in the wall region, as given by Black [6].

finds the same evolution of the flow field, but with a certain phase-shift in the x-direction. At a fixed position a gradual deceleration will be observed, until the next local instability passes by. As a consequence of a local instability the velocity profile $u(y, t)$ shows an "overshoot", followed by a slow relaxation. Assuming λ_x and U_c to be constant, the velocity profile $u(y, t)$ is periodical with period $T_b = \lambda_x/U_c$. Intersection (i) in Fig. 3 corresponds to Fig. 1. The interaction of neighbouring "streaks", supposed to be weak and negligible, results in the weak vorticity component; hence intersection (ii) in Fig. 3 corresponds to Fig. 2.

In the following sections we derive and solve the equations for the flow field in the time interval between local instabilities. Our model for the wall region is inspired by the surface renewal model and based upon the picture given by Black. This implies that we modify the surface renewal model by accounting for the periodicity in the flow direction and the convective transport of momentum. The temperature field in the wall region, in the case of a uniform wall temperature, is also calculated on the basis of this model.

2. MATHEMATICAL MODEL

In view of what is said in the previous section the velocity-field in the wall region is thought to be composed of two components:

1. A time dependent and periodical movement, which reflects itself in the observed coherence.

2. A time dependent and disordered movement, i.e. the fluctuations superimposed on the ordered movement.

During the quiet stage the ordered movement is gradually decelerated. This gradual deceleration continues until an unstable velocity profile arises. By this instability the already present velocity fluctuations are magnified, resulting in an intensive exchange of mass, momentum and heat and a rapid acceleration of the ordered movement. We therefore introduce the following decomposition:

$$\begin{aligned} \mathbf{u}(\mathbf{x}, t) &= \tilde{\mathbf{u}}(\mathbf{x}, t) + \mathbf{u}''(\mathbf{x}, t) \\ p(\mathbf{x}, t) &= \tilde{p}(\mathbf{x}, t) + p''(\mathbf{x}, t) \\ \theta(\mathbf{x}, t) &= \tilde{\theta}(\mathbf{x}, t) + \theta''(\mathbf{x}, t). \end{aligned} \tag{2.1}$$

Here the tilde denotes the ordered movement, being time dependent and varying periodically with a time scale $\tilde{T}$ equal to the burst period, T_b. The fluctuations $\mathbf{u}''$, p'' and θ'' vary at a time scale T_i, equal to the average duration of the burst and sweep event. Blackwelder and Kaplan [7] found in their experiments for the ratio of these time scales: $T_i/\tilde{T} \approx 0.05$. We shall calculate the quantities $\tilde{\mathbf{u}}$, $\tilde{p}$ and $\tilde{\theta}$ on the basis of the equations for an incompressible fluid in the form

$$\begin{aligned} &\nabla \cdot \mathbf{u} = 0 \\ &\frac{\partial \mathbf{u}}{\partial t} + \mathbf{u} \cdot \nabla \mathbf{u} = -\frac{1}{\rho} \nabla p + \nu \nabla^2 \mathbf{u} \\ &\frac{\partial \theta}{\partial t} + \mathbf{u} \cdot \nabla \theta = a \nabla^2 \theta. \end{aligned} \tag{2.2}$$

An (x, z)-plane is thought to be divided in "streaks", in which, apart from a phase shift, the same processes take place. We shall neglect their mutual interaction as caused by the secondary vorticity component. This means, that the evolution of the velocity field, $\tilde{u}$, in a "streak" between two local instabilities is an essentially two-dimensional event. For this reason variations in the z-direction will not be considered, hence $\tilde{\mathbf{u}} = [\tilde{u}(x, y), \tilde{v}(x, y)]$ and $\tilde{w} = 0$. Next we average the equations over a time interval τ, with $\tau \ll T_b$ and $\tau \gg T_i$, an operation again denoted by a tilde. Averaging quantities like $\tilde{u}$ will not alter them and averaging fluctuations, like u'', is supposed to give zero. Applying this averaging scheme results in

$$\begin{aligned} &\nabla \cdot \tilde{\mathbf{u}} = 0 \\ &\frac{\partial \tilde{\mathbf{u}}}{\partial t} + \tilde{\mathbf{u}} \cdot \nabla \tilde{\mathbf{u}} = -\frac{1}{\rho} \nabla \tilde{p} + \nu \nabla^2 \tilde{\mathbf{u}} - \nabla \cdot (\widetilde{\mathbf{u}''\mathbf{u}''}) \\ &\frac{\partial \tilde{\theta}}{\partial t} + \tilde{\mathbf{u}} \cdot \nabla \tilde{h} = a \nabla^2 \tilde{\theta} - \nabla \cdot (\widetilde{\mathbf{u}''\theta''}). \end{aligned} \tag{2.3}$$

The above equations have to be viewed as time dependent Reynolds' equations, with $\widetilde{\mathbf{u}''\mathbf{u}''}$ and $\widetilde{\mathbf{u}''\theta''}$ respectively as representing the "turbulent" transfer of momentum and heat. As in classical turbulence theories we meet a closure-problem. This problem is solved by taking into account the picture emerging from the visualization studies. First of all turbulent exchange mainly takes place during a burst and sweep. During the quiet period we shall neglect it. Secondly we simplify the local activity of burst and sweeps, by supposing that they are only active for discrete and

equally spaced values of $x = U_c t + n\lambda_x$ with $n = 0, 1, 2, \ldots$ Next we assume velocity and temperature profiles to be known immediately after a burst and sweep. So for $n\lambda_x < x - U_c t < (n+1)\lambda_x$ the terms $\nabla\cdot(\mathbf{u}''\mathbf{u}'')$ and $\nabla\cdot(\mathbf{u}''\theta'')$ in equations (2.3) are neglected and the following boundary conditions are imposed:

$$\tilde{u}(x,0,t) = 0,\ \tilde{u}[x = U_c t + (n+1)\lambda_x, y] = u_0(y)$$
$$\tilde{\theta}(x,0,t) = \theta_w,\ \tilde{\theta}[x = U_c t + (n+1)\lambda_x, y] = \theta_0(y). \tag{2.4}$$

Further we assume that, moving with the convective velocity U_c in the main flow direction, a stationary pattern is observed. Hence

$$\tilde{u}(x,y,t) = \tilde{u}(x - U_c t, y) \tag{2.5}$$

with similar equations for $\tilde{p}$ and $\tilde{\theta}$.

Substituting (2.4) in equations (2.3), applying a boundary-layer approximation to these equations and introducing the following transformation of variables

$$x_c = U_c t - x - (n+1)\lambda_x,\ u_c = -(\tilde{u} - U_c)$$
$$v_c = \tilde{v},\ \theta_c = \theta_w - \tilde{\theta} \tag{2.6}$$

we obtain the following equations, which hold for $0 < x_c < \lambda_x$:

$$\frac{\partial u_c}{\partial x_c} + \frac{\partial v_c}{\partial y} = 0$$
$$u_c\frac{\partial u_c}{\partial x_c} + v_c\frac{\partial u_c}{\partial y} = -\frac{1}{\rho}\frac{\mathrm{d}\tilde{p}}{\mathrm{d}x_c} + \nu\frac{\partial^2 u_c}{\partial y^2} \tag{2.7}$$
$$u_c\frac{\partial \theta_c}{\partial x_c} + v_c\frac{\partial \theta_c}{\partial y} = a\frac{\partial^2 \theta_c}{\partial y^2}$$

with the boundary conditions:

$$u_c(0,y) = U_c - u_0(y),\ \mathbf{u}_c(x,0) = \mathbf{0}$$
$$\theta_c(0,y) = \theta_w - \theta_0(y),\ \theta_c(x,0) = 0. \tag{2.8}$$

As a consequence of the boundary layer approximation a boundary condition for the $\tilde{v}$-component for $x = U_c t + (n+1)\lambda_x$, or $x_c = 0$, can no longer be imposed. The pressure gradient $\mathrm{d}\tilde{p}/\mathrm{d}x_c$ is determined by the velocity field outside the wall region or sub-boundary layer.

The original variables, which are periodical in the x-direction with a wave length λ_x, are related to the new variables according to:

$$\tilde{u}(x,y,t) = U_c - u_c(U_c t - x, y)$$
$$\tilde{v}(x,y,t) = v_c(U_c t - x, y) \tag{2.9}$$
$$\tilde{\theta}(x,y,t) = \theta_w - \theta_c(U_c t - x, y).$$

3. EVALUATION OF PARAMETERS

Before we can calculate the velocity- and temperature fields between two local instabilities from equations (2.7) we have to make suitable choices for $u_0(y)$, $\theta_0(y)$, U_c and $\mathrm{d}\tilde{p}/\mathrm{d}x_c$.

The choice of $u_0(y)$ and $\theta_0(y)$ is based on the surface renewal concept, i.e. the idea that during a burst and sweep the fluid in the wall region is replaced by fluid from the turbulent core, which is characterized by a logarithmic velocity profile. Just as in the surface renewal model we take for $u_0(y)$ a uniform profile u_0 and similarly for $\theta_0(y)$ a uniform value θ_0. Since the values of u_0 and θ_0 cannot be derived from the visualisation studies we estimate u_0 from the empirical profile $u^+ = 5.5 + 2.5\ln(y^+)$ for $y^+ = 30$, 40, 50 and 60, while the θ_0 values are adopted from the experimental data of Blom [8] for the same y^+ values.

For U_c we choose the convective velocity as measured in the wall region. This velocity is higher than the local mean fluid velocity (cf. Hinze [9]). Empirically it is found that the convective velocity equals the mean velocity for $y/\delta = 0.24$. Because for this position $\tilde{u} = 0.8U_\infty$ we take $U_c = 0.8U_\infty$.

Little is known about the pressure field in the wall region. Willmarth and Wooldridge [10] have performed measurements on the pressure fluctuations at the wall. They found for the RMS value $\langle\overline{p'^2}\rangle^{1/2} = 3\rho v^{*2}$. Taking this RMS value as characteristic for the pressure fluctuations, and the distance between two local instabilities, $\lambda_x = U_c T_b$, as the proper length scale we estimate that the pressure gradient in the wall region $\mathrm{d}\tilde{p}/\mathrm{d}x_c$ will be of the order $3\rho v^{*2}/U_c T_b$, which turns out to be small compared to the viscous force. Therefore we neglect this internal pressure gradient.

For choosing T_b we use the following empirical relation found by Rao *et al.* [11]:

$$v^{*2}T_b/\nu = 0.65Re_{\delta_2}^{0.75},$$
$$\text{for } 1000 < Re_{\delta_2} < 3500. \tag{3.1}$$

In reality the burst period at a fixed position shows a random variation around a stable average, denoted by T_b. It is noteworthy that T_b, scaled on the friction velocity v^* and the kinematic viscosity, depends on $Re_{\delta_2} = U_\infty\delta_2/\nu$, and is not a constant for the wall region. This indicates a coupling between the wall region and the outer region of the boundary layer.

4. SOLUTION OF THE EQUATIONS

With $u_0(y) = u_0$, $\theta_0(y) = \theta_0$ and $\mathrm{d}\tilde{p}/\mathrm{d}x_c = 0$ it is possible to find similarity solutions for u_c and θ_c, similar to the laminar boundary-layer problem. Substitution of

$$f'(\eta) = u_c(x_c, y)/(U_c - u_0)$$
$$g(\eta) = \theta_c(x_c, y)/(\theta_w - \theta_0) \tag{4.1}$$

with $\eta = y[(U_c - u_0)/\nu x_c]^{1/2}$, in equations (2.7) renders

$$2f''' + ff'' = 0,\ \text{with } f(0) = 0;$$
$$f'(0) = U_c/(U_c - u_0) = a_1; \tag{4.2a}$$
$$\lim_{\eta\to\infty} f'(\eta) = 1$$

$$2g'' + Prfg' = 0,\ \text{with } g(0) = 0;\ \lim_{\eta\to\infty} g(\eta) = 1. \tag{4.2b}$$

For solving the ordinary differential equation (4.2a) we use a method similar to the one Blasius has used for the laminar boundary-layer problem (Schlichting [12]). Instead of introducing a power series for small values of η, we linearize (4.2a), because the condition $f'(0) = a_1 \neq 0$ makes the evaluation of the coefficients of

such a power series rather troublesome. From the boundary conditions for $\eta = 0$ it can be seen that for $\eta \to 0$ $f(\eta) = a_1\eta + \frac{1}{2}a_2\eta^2$ with $f''(0) = a_2$, which is unknown. Hence for small values of η, the approximate solution f_0 satisfies

$$2f_0''' + (a_1\eta + \tfrac{1}{2}a_2\eta^2)f_0'' = 0, \text{ with } f_0(0) = 0;$$
$$f_0'(0) = a_1; \quad f_0''(0) = a_2. \tag{4.3}$$

For large values of η, $f'(\eta)$ tends to 1, which implies, that $f(\eta) \simeq \eta + \beta$, where β is an integration constant. So we have for the asymptotic solution $f_\infty(\eta)$ the equation

$$2f_\infty''' + (\eta+\beta)f_\infty'' = 0 \quad \lim_{\eta\to\infty} f_\infty'(\eta) = 1 \tag{4.4}$$

These equations can directly be integrated:

$$f_0(\eta) = a_2 \int_0^\eta dq \int_0^q \exp\left[-\left(\frac{a_2}{12}p^3 + \frac{a_1}{4}p^2\right)\right]dp + a_1\eta \tag{4.5a}$$

$$f_\infty(\eta) = \gamma(\pi)^{1/2}\{(\eta+\beta)[\operatorname{erf}(\tfrac{1}{2}\eta+\tfrac{1}{2}\beta)-1] + [2/(\pi)^{1/2}]\exp[-(\eta+\beta)^2/4]\} + (\eta+\beta). \tag{4.5b}$$

The integral in (4.5a) does not have a simple primitive function. For numerical calculations we have used a Taylor series. The solution of $f_0(\eta)$ still contains the unknown boundary condition $f''(0) = a_2$. In the same way the solution of $f_\infty(\eta)$ contains two unknown integration constants β and γ, because we only have one boundary condition at our disposal. The 3 unknown parameters: a_2, β and γ are determined by requiring continuity of f, f' and f'' for a suitable η-value, where the inner and outer solutions meet. This supplies us with three non-linear equations, which are solved numerically.

The applied linearization of the differential equation (4.2a) implies that the zeroth order approximation for the large scale velocity $\tilde{u}$ reads as

$$\tilde{u} = (u_0 - U_c)a_2\eta, \quad \text{for} \quad 0 < \eta < \eta_1$$
$$\tilde{u} = (U_c - u_0)(a_1 - 1), \quad \text{for} \quad \eta > \eta_1.$$

Hence, in the zeroth approximation $\tilde{u}$ is continuous for $\eta_1 = (1-a_1)/a_2$, as shown in Fig. 4. The coupling of the inner and outer solutions of the first order approximation, given by equations (4.5), is done at $\eta_1 = (1-a_1)/a_2$, as well. Thus we find for $\tilde{u}(x, y, t)$ between two local instabilities:

$$\tilde{u}(x,y,t) = U_c - (U_c - u_0)f_0'(\eta), \text{ for } 0 \leqslant \eta \leqslant \eta_1$$
$$\tilde{u}(x,y,t) = U_c - (U_c - u_0)f_\infty'(\eta), \text{ for } \eta_1 \leqslant \eta < \infty. \tag{4.6}$$

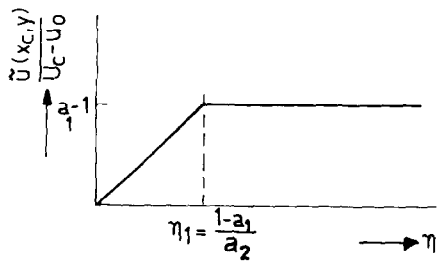

FIG. 4. Zeroth order approximation of $\tilde{u}$.

The equation for the temperature field (4.2b) is treated in the same way. We approximate f in (4.2b) as above. In this way an inner solution $g_0(\eta)$ and an outer solution $g_\infty(\eta)$ are found, which are matched at $\eta = \eta_1$ by requiring continuity of g and g'. The following approximate solution for $g(\eta)$ is found

$$g_0(\eta) = q_1 \int_0^\eta \exp\left[-Pr\left(\frac{a_2}{12}p^3 + \frac{a_1}{4}p^2\right)\right]dp \qquad 0 \leqslant \eta \leqslant \eta_1$$

$$g_\infty(\eta) = q_2\left(\frac{\pi}{Pr}\right)^{1/2}\{\operatorname{erf}[(\tfrac{1}{2}\eta+\tfrac{1}{2}\beta)(Pr)^{1/2}]-1\}+1 \qquad \eta_1 \leqslant \eta \leqslant \infty. \tag{4.7}$$

The parameters q_1 and q_2 are determined by the two matching conditions. The applied solution method was checked with a fully numerical integration for one value of a_1. From this check it was concluded that the applied method is satisfactory. The deviations kept within a range of $\pm 0.5\%$.

5. COMPARISON WITH EXPERIMENT

From (4.6) the instantaneous and time averaged wall shear stress is obtained. To find time averages, we can restrict ourselves to one period.

$$\bar{\tau}_w = \frac{1}{T_b}\int_0^{T_b} \tau_w\,dt = -2\frac{a_2\mu U_c}{a_1}(a_1\nu T_b)^{-1/2}. \tag{5.1}$$

Nondimensionalizing this calculated value of $\bar{\tau}_w$, with v^*, the experimental friction velocity, we have

$$\bar{\tau}_w/\rho v^{*2} = -2a_2\left(\frac{U_c}{v^*}\right)\left(\frac{v^{*2}T_b}{\nu}\right)^{-1/2} a_1^{-3/2}. \tag{5.2}$$

Equation (5.2) contains three parameters, viz: the convective velocity U_c, the boundary condition u_0 and the period T_b, parameters we already have chosen. With the aid of the empirical formula $(v^*/U_\infty)^2 = 0.012Re_{\delta_2}^{-0.25}$ (Hinze [9]) the ratio between the theoretical and experimental values of $\bar{\tau}_w$ appears to be dependent of Re_{δ_2}. This ratio as a function of Re_{δ_2} is plotted in Fig. 5 for different values of u_0/v^*, corresponding to the different choices of u_0 (at $y^+ = 30, 40, 50, 60$) mentioned in Section 3.

Although one cannot speak of an exact accordance—in that case the calculated ratio should be independent of Re_{δ_2} and equal to 1—the calculated ratio is only weakly dependent of Re_{δ_2} and has the right order of magnitude.

Further we have calculated the evolution of the velocity profile $\tilde{u}(y, t)$ for a fixed x-position during one period. Nondimensionalizing $\tilde{u}(y, t)$ with v^* and T_b we have

$$\frac{\tilde{u}}{v^*} = \frac{U_c}{v^*} - \frac{(U_c - u_0)}{v^*}f'(\eta)$$
$$\eta = y^+\left[a_1\frac{v^{*2}T_b}{\nu}\frac{t}{T_b}\right]^{-1/2}. \tag{5.3}$$

Equation (5.3) still contains the undetermined parameter Re_{δ_2}. We have chosen that Re_{δ_2}-value for which

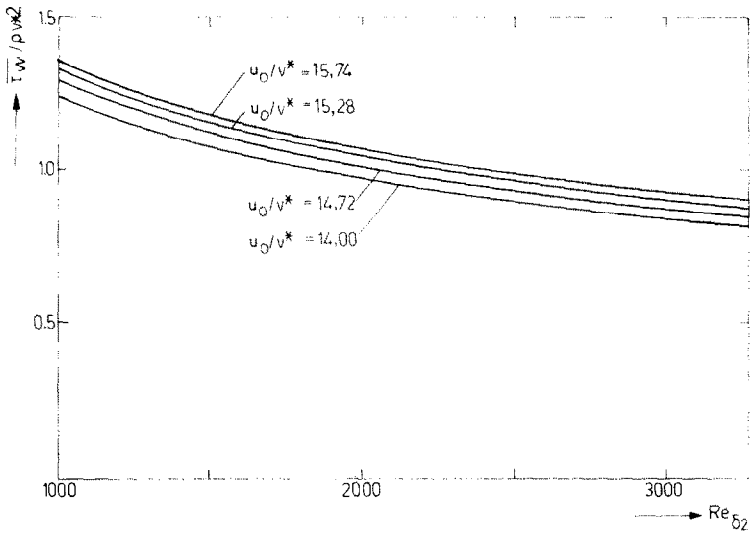

FIG. 5. The ratio of theoretical and experimental mean wall stress.

$\bar{\tau}_w/\rho v^{*2} = 1$. This implies, that we have made a certain choice for the period T_b, because U_∞/v^* is only weakly dependent on Re_{δ_2}. In Fig. 6 one finds $\bar{u}/v^*$ as a function of y^+ for several values of t/T_b.

Finally we shall compare our model with the law of the wall $\bar{u}/v^* = u^+(y^+)$. In our model the time averaged velocity profile is found by averaging $\hat{u}$ over one period. Again we have chosen that period, i.e. that Re_{δ_2}-value, for which the calculated value $\bar{\tau}_w$ equals the experimental wall stress ρv^{*2}. Nondimensionalized with v^* and ν the result is:

$$u^+(y^+) = \frac{U_e}{v^*}\left\{1 + \frac{2(y^+)^2}{a_1^2 v^{*2} T_b/\nu} \times \int_{-\infty}^{y^+\left(a_1 \frac{v^{*2}T_b}{\nu}\right)^{1/2}} \frac{f'(\eta)}{\eta^3}\,d\eta\right\}. \quad (5.4)$$

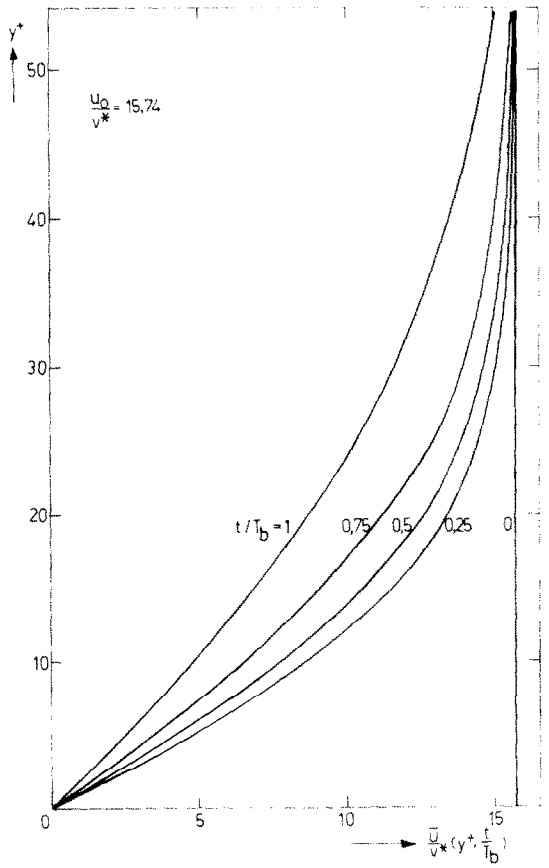

FIG. 6. The evolution of the large scale velocity component $\hat{u}$ between two local instabilities. The moment just after the occurrence of a burst and sweep corresponds to $t/T_b = 0$.

The law of the wall is widely known and accepted, but it is hard to find a generally accepted form. We used the empirical formula of Spalding [8]

$$y^+ = u^+ + 0.1108\left\{\exp(0.4u^+) - \sum_{n=0}^{3}\frac{(0.4u^+)^n}{n!}\right\}.$$

Blom [8] has shown that the Spalding formula should not be taken too rigidly. Comparing the experimental data of a number of authors a considerable scatter is found (cf. Fig. 7). Table 1 gives the numerical values of various parameters.

Table 1. Values of u_0/v^* and the corresponding values of Re_{δ_2}, a_1 and $v^{*2}T_b/\nu$

u_0/v^*	Re_{δ_2}	a_1	$v^{*2}T_b/\nu$
14.00	1845	3.5940	183
14.72	2071	3.9680	200
15.82	2256	4.3139	213
15.74	2414	4.6441	224

The temperature field

With the solution (4.7) for $g(\eta)$ we can calculate the mean heat flux at the wall, the development of the temperature profile after a burst and sweep and time averaged temperature profiles.

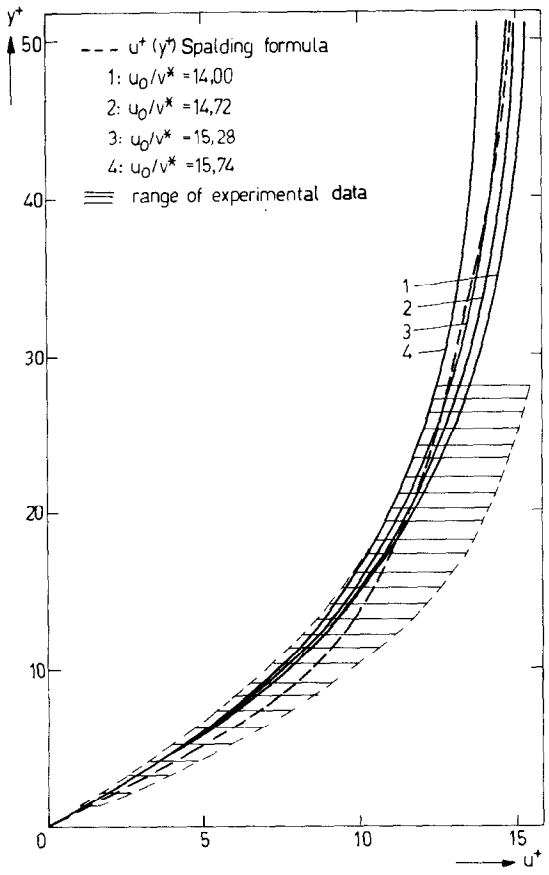

FIG. 7. The calculated mean velocity profiles $u^+(y^+)$ for different values of u_0 (curves 1–4), as compared with Spalding's profile. Range of experimental data according to Blom [8].

The mean heat flux at the wall is found from:

$$\bar{q}_w = \frac{1}{T_b}\int_0^{T_b} q_w \,\mathrm{d}t = 2\lambda\nu^{-1/2}(\theta_w-\theta_0) \times (U_c-u_0)^{1/2}(U_c T_b)^{-1/2} g'(0). \quad (5.5)$$

The theoretical mean heat flux is compared to experiment in the same way as was done for the mean wall stress. We nondimensionalize (5.5) with v^* and the experimental friction temperature defined as $\theta^* = q_w/(\rho c_p v^*)$, which results in

$$\bar{q}_w/(\rho c_p v^*\theta^*) = \frac{2}{Pr}\frac{(\theta_w-\theta_0)}{\theta^*} a_1^{-1/2}\left(\frac{v^{*2}T_b}{\nu}\right)^{-1/2} g'(0). \quad (5.6)$$

The ratio between the theoretical and the experimental values of $\bar{q}_w/(\rho c_p v^*\theta^*)$ turns out to be also dependent on Re_{δ_2}, as can be seen in Fig. 8. The development of the large scale temperature profile between the passage of two local instabilities is calculated and nondimensionalized with θ^*.

$$\frac{\tilde{\theta}(y^+, t/T_b)}{\theta^*} = \frac{\theta_w-\theta_0}{\theta^*} g(\eta). \quad (5.7)$$

It is clear, that the parameter Re_{δ_2}, which occurs in equation (5.7) has already been determined by the velocity field. Results are shown in Fig. 9. The time averaged temperature profile is found in the same way as the time averaged velocity profile, viz. *bij* averaging $\tilde{\theta}$ over one period. In nondimensional form this renders

$$\frac{\bar{\theta}}{\theta^*} = \theta^+(y^+) = \frac{(\theta_w-\theta_0)}{\theta^*}\frac{2(y^+)^2}{a_1 v^{*2}T_b/\nu} \times \int_\infty^{y^+\left(a_1\frac{v^{*2}T_b}{\nu}\right)^{-1/2}} -\frac{g(\eta)}{\eta^3}\,\mathrm{d}\eta. \quad (5.8)$$

In Fig. 10 the calculated mean temperature profile is compared with the measurements of Blom for several values of θ_0/θ^*.

6. COMPARISON WITH THE SURFACE RENEWAL MODEL

The mathematical formulation of the surface renewal model, given by equation (1.1) has the solution:

$$\tilde{u}(y, t) = u_0 \,\mathrm{erf}[y/2(\nu t)^{1/2}]. \quad (6.1)$$

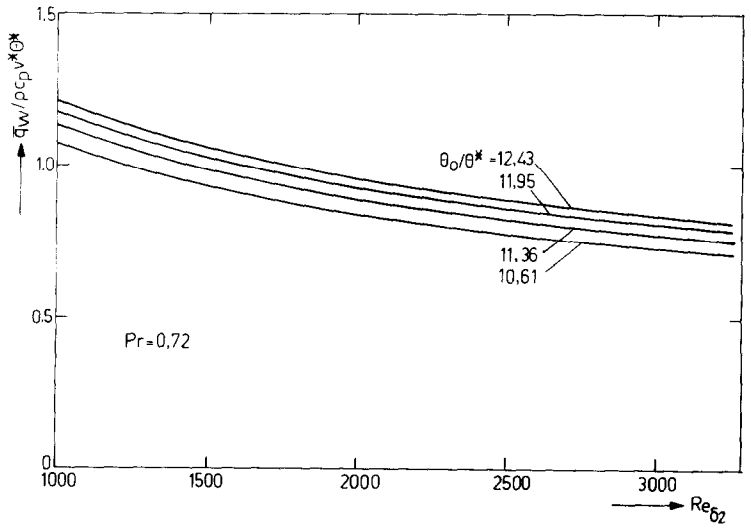

FIG. 8. The ratio of theoretical and experimental mean heat fluxes at the wall. The values of θ_0/θ^* have been estimated from the experimental temperature profile of Blom [8] at $y^+ = 30, 40, 50$ and 60.

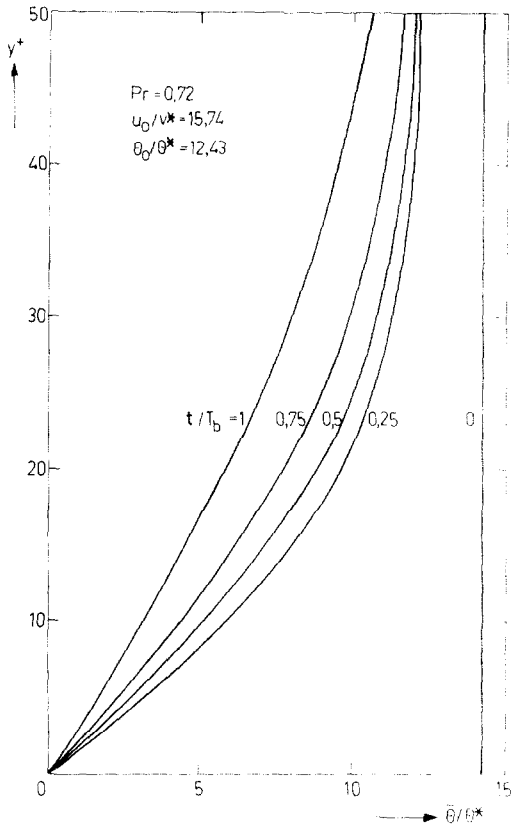

FIG. 9. The development in time of the temperature profile during one period.

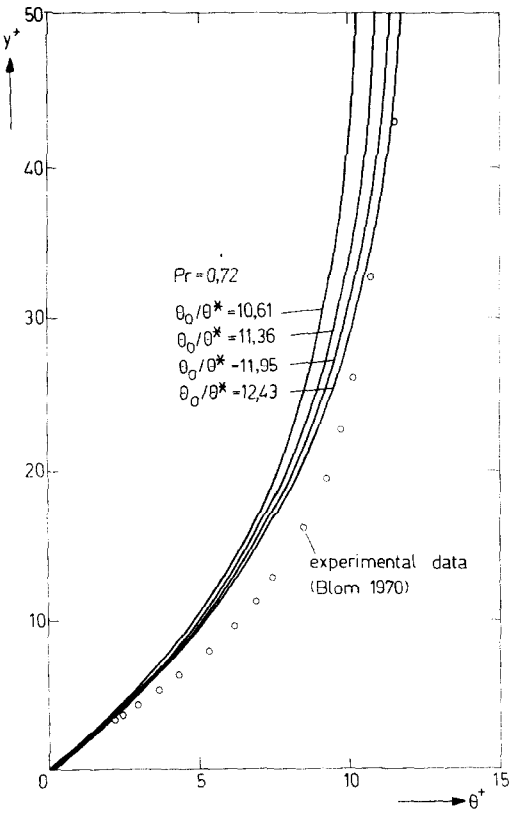

FIG. 10. The calculated mean temperature profiles $\theta^+(y^+)$.

The ratio of the calculated and experimental values of the mean wall stress $\bar{\tau}_w/\rho v^{*2}$ and the time averaged velocity profile $u^+(y^+)$, for a recurrence period of the surface renewal equal to T_b, take the forms:

$$\frac{\bar{\tau}_w}{\rho v^{*2}} = \frac{2}{(\pi)^{1/2}} \frac{u_0}{v^*} \left(\frac{v^{*2} T_b}{\nu} \right)^{-1/2}$$

$$u^+(y^+) = \frac{u_0}{v^*} \left\{ (2H^2+1)\,\mathrm{erf}(H) + \frac{2H}{(\pi)^{1/2}} e^{-H^2} - 2H^2 \right\} \tag{6.2}$$

$$\text{with } H = \frac{y^+}{2(v^{*2} T_b/\nu)^{1/2}}.$$

In this case $\bar{\tau}_w/\rho v^{*2}$ is Re_{v^*}-dependent via the period T_b as well. We have compared this ratio with our results for one value of u_0/v^* (other values leading to similar results). This is shown in Fig. 11.

From this figure it can be seen, that the ratio calculated with our model decreases less steeply than for the surface renewal model, but the most obvious difference is that we find smaller values, which means that the effect of the convective transport of momentum is not negligible in the wall region. Nevertheless, also in the surface renewal model a Re_{v^*} value can be found for which $\bar{\tau}_w = \rho v^{*2}$. The corresponding value of T_b is chosen to evaluate the time averaged velocity profile $u^+(y^+)$ in (6.2). We have plotted the mean velocity profiles calculated with our model and the surface renewal model in Fig. 12.

At first sight no large impact of the convective transport of momentum on the mean velocity profile seems to occur. This, however, is hidden by the choice of the averaging time T_b. To arrive at the exact value of the mean wall stress we have to use smaller values of Re_{v^*}, or the averaging time in our model, than in the surface renewal model, as can be seen from Table 2.

Table 2. The Re_{v^*} values and corresponding averaging times in both models

Surface renewal model			Present model	
u_0/v^*	Re_{v^*}	$v^{*2}T_b/\nu$	Re_{v^*}	$v^{*2}T_b/\nu$
14.00	2790	250	1845	183
14.72	3190	276	2071	200
15.28	3524	297	2256	213
15.74	3814	315	2414	224

7. DISCUSSION AND CONCLUSIONS

With the discussed intermittent and periodic model for the wall region of a turbulent boundary layer we have been able to calculate the mean wall stress $\bar{\tau}_w$, the time averaged velocity profile u^+, the mean heat flux at the wall q_w and the time averaged temperature profile θ^+. From a comparison between the theoretical values and experimental data we conclude that one can speak of a reasonable accordance, as shown by Figs. 5, 7, 8 and 10. Therefore it seems justified to state that in our model of the exchange processes in the wall region the most essential features are reflected, at least for that

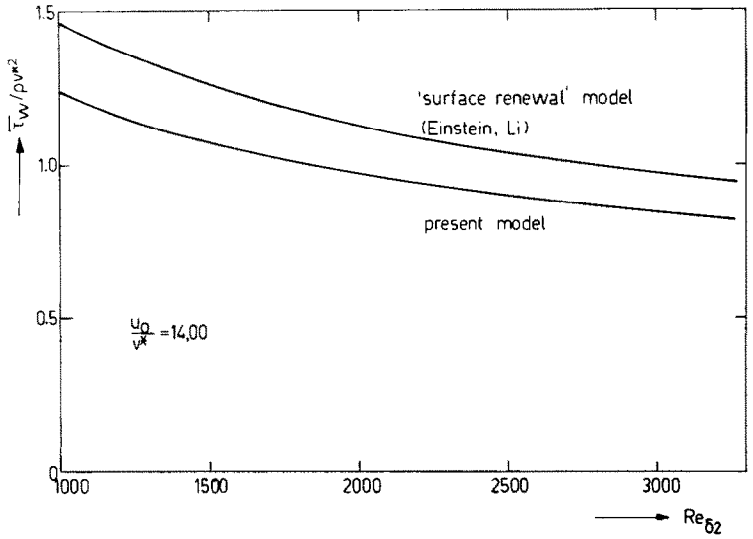

FIG. 11. The ratio of the theoretical and experimental mean wall stresses for the surface renewal model and the present model as a function of Re_{δ_2}.

range of Re_{δ_2} values, that corresponds to the visualization studies, whereupon our model ultimately is based: $1000 < Re_{\delta_2} < 3500$. This does not mean, that certain refinements should not be possible, particularly regarding the choice for the velocity- and temperature profiles after a burst and sweep $\tilde{u}_0(y)$ and $\tilde{\theta}_0(y)$, and the period T_b. For $u_0(y)$ and $\tilde{\theta}_0(y)$ we have

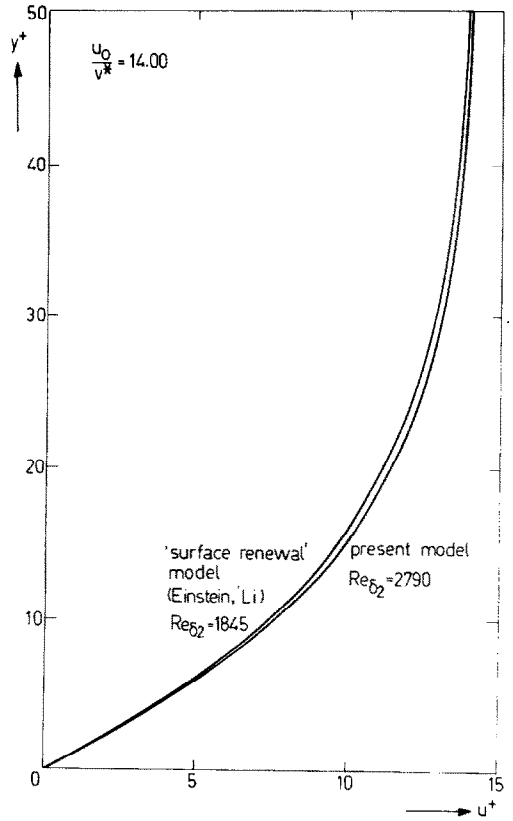

FIG. 12. The mean velocity profile according to the present model and the surface renewal model.

chosen uniform profiles, but it is clear that very close to the wall this is rather unrealistic. Concerning the period T_b we should have accounted for the fact that the burst-period T_b is statistically distributed. Should anything be known about the corresponding distribution function, then we could incorporate this in the procedure for obtaining averaged quantities. Nevertheless we believe, that, discarding the difficulties to find more reliable data for $\tilde{u}_0(y)$, $\theta_0(y)$ and the distribution of T_b, these refinements would not change our model essentially.

The qualitative agreement between the development of the profile $\tilde{u}(y, t)$ between two local instabilities (cf. Fig. 6) and experimental results is less encouraging. Our model does describe the gradual deceleration of the fluid in the wall region, but not the creation of an inflexional zone in the velocity profile, which is characteristic for the onset of the next burst and sweep. Our model cannot explain the occurrence of the burst mechanism. We have assumed the periodicity in the wall region *a priori* and adopted the burst period from empirical data. The fact that the present model does not describe the generation of an inflexional zone, can only mean that we have not incorporated the responsible mechanism in the model. We mention two possibilities, which could account for this mechanism.

1. The pressure gradient $d\bar{p}/dx_c$ in the wall region between two bursts and sweeps has been neglected. We emphasize that we only consider pressure fluctuations generated by the outer part of the total turbulent boundary layer. It is a well known fact that a positive pressure gradient can cause flow separation. So the pressure field generated in the whole turbulent boundary layer could, via the mechanism of flow separation in the sub-boundary layer, be able to maintain the bursts and sweeps. We have estimated the pressure gradient (Section 3) to be $(d\bar{p}/dx_c) \simeq 3\rho v^{*2}/U_c T_b$. The effect of this pressure gradient has been evaluated by

applying a Pohlhausen approximation [12] on the equations for the sub-boundary layer (2.7) including the pressure gradient. It was found that the estimated pressure gradient is far too weak to give an inflexional zone at $y^+ = 20$ to 30 after a time interval T_b. That is why we reject the pressure gradient as the possible mechanism for the maintenance of the bursts and sweeps.

2. The "streak" structure becomes predominant for $y^+ < 40$ to 50, thus at the upper edge of the buffer region. This "streak" structure is accompanied by a weak vorticity component in the main flow direction (cf. the Introduction). In our model the phenomena in the wall region take place in "streaks" in a (x, z)-plane without mutual interference between such "streaks". As revealed by the visualization studies of Kline *et al.* there is an interaction between two neighbouring "streaks", leading to pairs of counter-rotating vortices in a (y, z)-plane. These have been neglected in deriving the equations for the large scale velocity field. This secondary motion might be responsible for the creation of the inflexional zone in the large scale velocity profile $\bar{u}(y, t)$, just before the occurrence of a burst. Stuart [13] has shown quantitatively, that in the transition from laminar to turbulent flow, where the cited structure of "streaks" accompanied by pairs of counter-rotating vortices is also observed, this mechanism is able to create an inflexional zone in the low speed region. In his calculations he started with an assumption about the counter-rotating vortices, while viscosity was neglected. However, should this concept be applied to the wall region, in order to find the time necessary to create an inflexional zone at $y^+ = 20$–30, two serious difficulties will be encountered:

(i) because we are considering the wall region, viscosity can not be neglected;

(ii) the strength of these pairs of counter-rotating vortices should be derived from empirical results, which can hardly be found.

REFERENCES

1. S. J. Kline, W. C. Reynolds, F. A. Schraub and P. W. Rundstadler, The structure of turbulent boundary layers, *J. Fluid Mech.* **30**, 741–773 (1967).
2. H. T. Kim, S. J. Kline and W. C. Reynolds, The production of turbulence near a smooth wall in a turbulent boundary layer, *J. Fluid Mech.* **50**, 133–160 (1970).
3. E. R. Corino and R. S. Brodkey, A visual investigation of the wall region in turbulent flow, *J. Fluid Mech.* **37**, 1–30 (1969).
4. H. A. Einstein and H. Li, The viscous sublayer along a smooth boundary, *J. Engng Mech. Div. Am. Soc. Civ. Engrs* **82**(EM2), 945 (1956).
5. T. J. Hanratty, Turbulent exchange of mass and momentum with a boundary, *A.I.Ch.E. Jl* **2**, 359–362 (1956).
6. T. J. Black, An analytic study of the measured wall pressure field under supersonic turbulent boundary layers, NASA CR-888 (1968).
7. R. F. Blackwelder and R. E. Kaplan, The intermittent structure of the wall region of the turbulent boundary layer, Univ. S. Calif. Rep. USCAE. 1–22 (1972).
8. J. Blom, An experimental determination of the turbulent Prandtl number in a developing temperature boundary layer, Dissertation, Eindhoven Univ. of Techn. (1970).
9. J. O. Hinze, *Turbulence*, 2nd edn. McGraw-Hill, New York (1975).
10. W. W. Wilmarth and C. E. Wooldridge, Measurements of the fluctuating pressure at the wall beneath a thick turbulent boundary layer, *J. Fluid Mech.* **14**, 187–210 (1962).
11. K. Narahari Rao, R. Narasimha and M. A. Badri Narayanan, The "bursting" phenomenon in a turbulent boundary layer, *J. Fluid Mech.* **48**, 339–352 (1971).
12. H. Schlichting, *Grenzschicht Theorie*. G. Braun, Karlsruhe (1958).
13. J. T. Stuart, The production of intense shear layers by vortex stretching and convection, AGARD Rep. 514 (1965).

MODELE PERIODIQUE INTERMITTENT POUR LA ZONE PARIETALE D'UNE COUCHE LIMITE TURBULENTE

Résumé—Des études de visualisation de l'écoulement turbulent au voisinage d'une paroi montrent que des intervalles de temps courts avec une forte activité turbulente (appelés éclatements et balayages) alternent avec des intervalles de plus longue durée où les effets visqueux prédominent. Ces phénomènes montrent une quasi périodicité dans l'espace et dans le temps. L'évolution des profils de vitesse et de température est calculée pour une période de temps à partir des équations de la couche limite bidimensionnelle pour la région $0 < y^+ < 40$. L'effet combiné d'un éclatement et d'un balayage est supposé créer des profils uniformes de vitesse et de température au début de la période. Dans cette idée, le modèle présenté est semblable au modèle du renouvellement de surface. Les paramètres intervenant dans les équations et les conditions aux limites sont dérivés de l'expérience. Le modèle donne convenablement les profils de vitesse et de température dans la région pariétale ainsi que les flux de chaleur et de quantité de mouvement.

EIN PERIODISCH INTERMITTIERENDES MODELL FÜR DIE WANDREGION EINER TURBULENTEN GRENZSCHICHT

Zusammenfassung—Studien bei der Sichtbarmachung turbulenter Strömungen in der Nähe von Wänden haben gezeigt, daß sich kurzzeitige Intervalle mit starker Turbulenz (sogenanntes Wirbelplatzen und Mitreißen) mit Intervallen von viel längerer Dauer abwechseln, bei welchen die Viskosität einen überwiegenden Einfluß ausübt. Diese Phänomene zeigen eine Quasi-Periodizität in Raum und Zeit. Die Ausbildung der Geschwindigkeits- und Temperaturprofile wird für eine Zeitperiode mit Hilfe einer zweidimensionalen laminaren Grenzschichtgleichung für das Gebiet $0 < y^+ < 40$ berechnet. Es wird

angenommen, daß dieser kombinierte Wirbelplatz- und Mitreißeffekt die Ausbildung eines mittleren Geschwindigkeits- und Temperaturprofils am Anfang der Periode ermöglicht. In dieser Beziehung entspricht dieses Modell dem Oberflächenerneuerungs-Modell. Die verschiedenen Parameter, die in den Gleichungen und Randbedingungen auftreten, stammen aus Experimenten. Nach diesem Modell lassen sich Geschwindigkeits- und Temperaturprofile in Wandnähe sowie Wärmeströme und Bewegungsgrößen an der Wand ziemlich gut vorausberechnen.

МОДЕЛЬ ЯВЛЕНИЯ ПЕРЕМЕЖАЕМОСТИ В ПРИСТЕННОЙ ОБЛАСТИ ТУРБУЛЕНТНОГО ПОГРАНИЧНОГО СЛОЯ

Аннотация — Визуальные исследования турбулентного течения вблизи стенки показали, что краткие периоды сильной турбулентной активности (так называемые всплески и выносы) чередуются с гораздо более длительными периодами, в которых преобладают эффекты вязкости. Это явление чередования носит квазипериодический характер в пространстве и времени. В работе представлены результаты профилей скорости и температуры для одного временного интервала по уравнениям для двухмерного ламинарного пограничного слоя в диапазоне $0 < y^+ < 40$. Различные входящие в уравнения параметры и граничные условия получены из экспериментов. Показывается, что наложение всплесков и выносов приводит к однородности профилей скорости и температуры в начале временного интервала. В этом отношении предлагаемая модель аналогична модели обновления поверхности. Модель позволяет довольно точно рассчитать профили скорости и температуры в пристенной области, а также потоки тепла и количества движения на стенке.